ICONHIC 2016
1st International Conference on Natural Hazards & Infrastructure
28-30 June, 2016, Chania, Greece

Landslide triggering modeling in Switzerland

Ahoura Jafarimanesh[1], Arnaud Mignan & Domenico Giardini

Institute of Geophysics, ETH Zürich, Switzerland

ABSTRACT

Triggered chains of events and their combined impact on infrastructures may yield unsuspected consequences (e.g., increased likelihood of hydropower dam mal-functions, increased damage around geo-energy exploitation sites). Here we present a simple cellular automaton to simulate landslide footprints triggered by both rain and earthquakes. The method is based on the Sandpile model, which dynamics is controlled by the ground slope. Rain levels are approximated by ground water saturation and earthquake-landslide triggering is evaluated using the concept of Newmark displacement. That concept is then modified to estimate stable slopes during shaking at which locations the landslide stops. The cellular automaton is first tested in a virtual area where a parameter sensitivity analysis is made. Then it is tested in a region of Switzerland, where historic landslides triggered by earthquakes are known to have occurred.

Keywords: Landslide triggering, Multi-risks, Cellular automaton, Sandpile model

1. INTRODUCTION

Switzerland is prone to hazard interactions due to its mountainous landscape. Historical earthquakes are known to have triggered aftershocks, landslides, rock falls and avalanches, as well as lake tsunamis (e.g., Fritsche et al., 2012). Globally, dams are also subject to hazard interactions. Examples include cascading dam failures due to heavy rains (e.g., 1975 Banquiao dam, China) and dam overtopping due to landslides (e.g., 1963 Vajont dam, Italy). Potential hazard interactions at geo-energy production sites, on the other hand, have not so far been systematically addressed. With such focus, we decided to use cellular automata models for hazard interaction modeling in the Generic Multi-Risk (GenMR) framework of Mignan et al. (2014). A recent application of GenMR to a conceptual Alpine embankment dam for example showed that inclusion of hazard interactions increased the risk of dam failure although this increase remained below the established risk safety margins (Matos et al. 2016). The degree of dependency of critical infrastructures to the reliable function of the electrical network, which can be disrupted by dynamic risk and interactions of various hazards in dams and geothermal sites, shows the value of the present study. So far an innovative cellular automaton to simulate landslide footprints triggered by both rain and earthquakes has been developed (Sandpile model with dynamics controlled by ground slope, ground water saturation and concept of Newmark displacement). First tested in a virtual area where a parameter sensitivity analysis is made (e.g., Liu et al. 2015), it is further tested in a region of Switzerland (where historic landslides triggered by earthquakes occurred) for model validation.

[1] A.Jafarimanesh
Institute of Geophysics, ETH Zurich, Switzerland
Email: Jafarimanesh@erdw.ethz.ch

2. METHODOLOGY

To be flexible in the implementation of multi-risk processes (i.e. hazards interaction and dynamic risk), the following top-down approach to multi-risk analysis has been put into place (Fig. 1):

a. Abstract level: Development of multi-risk models using basic mathematical tools (here, cellular automaton);
b. Generic level ("Virtual City" concept): Testing of simplified (but realistic enough) multi-risk models (e.g., landslide triggering) in a controlled environment for benchmarking and parameter sensitivity analysis;
c. Site-specific level (Switzerland): Application of multi-risk models to real-site conditions, using existing topography, soil properties, building portfolios, etc.

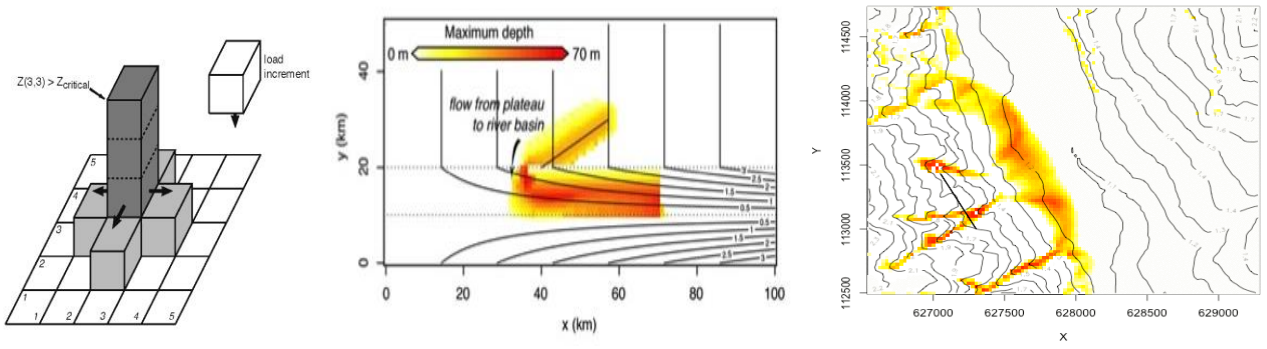

a **b** **c**

Figure 1. The three steps of the multi-risk approach. a: Concept of the Sandpile model in an infinite lattice; b: Cellular automaton tested in a virtual area; c: Cellular automaton tested in the Mattertal valley, Valais, Switzerland. Landslide footprints are represented in orange.

Specifically for the landslide-triggering model, a cellular automaton (CA) algorithm has been developed to simulate landslide footprints in a simple and transparent way. In order to switch from this abstract/conceptual level to a generic level, the concept of a "Virtual City" located in a hazardous virtual area is then used (Komendantova et al., 2014; Liu et al., 2015; Mignan et al., 2016). It is set in a 100 km by 100 km region where various geological and hydrological elements are defined. The topography of this virtual area is shown in Fig. 2a. It includes a volcano with an unstable slope in the north-eastern part, faults in the central and north-western part, a river basin in the southern sector and a coast on the western side. Due to this configuration, different types of the perils may occur, such as volcanic eruptions, landslides, earthquakes, fluvial floods, storms, sea submersion, etc. This virtual area is considered as a controlled environment where any multi-risk scenario can be defined and sensitivity analyses can be made following reasoned imagination (e.g. Mignan et al., 2016b). Even though the associated uncertainties may remain high, the virtual area concept can be considered as a playground, which allows running any type of multi-risk scenario where data may be lacking. A schematic representation of the virtual area threatened by various perils is shown in Fig. 2b.

We have used the CA concept as it represents an alternative to complicated differential equations or finite element methods for simulating complex multi-hazard events (e.g., earthquake-triggered landslide). CA has a long history in complex system modeling in which the values of cells in an array are updated in discrete steps according to a local rule (Pickover, 2009). In the context of natural hazards, the original concept of self-organized criticality introduced by Bak et al. (1987) has been further developed by Malamud and Turcotte (2000), among many others. They developed CA models based on the forest-fire, slider-block, and Sandpile models. In general, frequency-area distributions can then be used to estimate/calibrate (between models and observations) the severity of hazardous events and the probability of their occurrence in a given time period. Finally, these couples severity/probability can be used as an input to implement multi-risk analysis in a multi-risk framework such as GenMR (Mignan et al., 2014; Matos et al., 2016). Below, we briefly explain the basis for the creation of the CA model for the simulation of landslides triggered by rainfall and earthquakes.

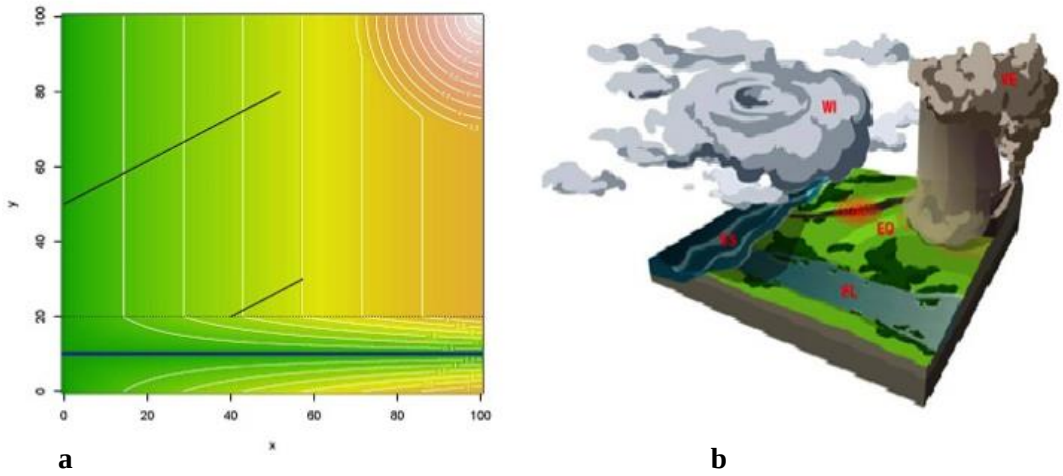

Figure 2. a: Virtual area topography defined to evaluate the relative roles of terrain slope (color gradient), water saturation due to the rainfall, and earthquakes (black segments); b: Principal sketch of the virtual area as developed within the MATRIX project, modified after Mignan et al. (2016). EQ, FL, SS, VE and WI stand respectively for earthquake, flood, sea submersion, volcanic eruption and wind.

2.1 Cellular automaton (CA) for landslide analysis

Landslides are viewed as a dynamic system based exclusively on local interactions between ground shaking parameters, physical characteristic of slope and ground water saturation by a rainfall level. To simulate the landslide footprint, which is potentially triggered by rain and earthquakes, a CA model based on the Sandpile model with dynamics controlled by ground slope, ground water saturation and concept of Newmark displacement has been developed. In this model discrete square cells represent space, whose initial states describe the current physical and mechanical characteristics of the portion of the slope (friction angle, effective cohesion, slab thickness, saturation, etc.). A CA environment is considered as a square grid of cells; we set out the boundary condition of the landslide displacement based on the Newmark displacement threshold. When the flow in an initial cell starts, the increments (or particles) accumulated on the cell get redistributed to the eight adjacent cells. This can lead to chain reactions with the occurrence of avalanche-type events. As an example of the application of the model in the real case studies, Malamud and Turcotte (2000) have shown that the non-cumulative frequency-area distribution of 11,000 landslides triggered by the 1994 Northridge earthquake, based on the study done by Harp and Jibson (1995) follows a rational correlation with the power law relation, and further can be retrieved in the sandpile model.

2.2 Review on Newmark slope stability analysis

In this section, we briefly explain the concept of dynamic slope stability and characterization of the seismic ground motion to be used as a primary estimate of the stable slope in our CA model defined for landslide triggering analysis. Based on the method developed by Jibson (1993) built upon the Newmark (1965) slope stability calculation for earthquake-induced landslide displacement, the dynamics of a slope can be quantified as the critical acceleration, a base acceleration needed to overcome the shear resistance of the slope and start the activation of the movement. Critical acceleration is calculated via Equation 1:

$$\mathrm{ac} = (\mathrm{Fs} - 1)\mathrm{gsin}\theta \qquad (1)$$

where a_c is the critical acceleration in terms of g (standard gravity), F_s is the static safety factor of slope (unit less), and θ is the angle of the horizontal surface to the sliding surface. The slope stability safety factor is expressed as the ratio of stabilizing forces to destabilizing forces and is shown in Equation 2 (Newmark, 1965).

$$FS = \{\frac{c}{\gamma sh} + [\gamma s(h - hw) + (\gamma s - \gamma w)hw]\cos\theta \tan\varphi\} / \gamma shsin\theta \qquad (2)$$

where C is the soil cohesion (N/m^2) , γ_s the soil weight (kg/m^3), γ_w the water weight (kg/m^3), θ then slope angle (°), and φ the internal friction angle (°); h accounts for the soil depth (m) and h_w is the height of the water table within the soil layer. The next task is to characterize the seismic ground motion (a_{max}) to be used in the Newmark method. At the time the Newmark method was introduced there were a few approaches to record the strong motion and therefore computation of the resources to conduct integration of Newmark method were rare. This was the reason of the popularity of simplified model to calculate the relative displacement based on Newmark (1965). To calculate the peak ground acceleration (PGA), we follow here the procedure described by Akkar and Bommer (2014), which suggests Equation 3 to calculate the pseudo spectral acceleration (PSA) in the logarithmic scale:

$$\log(PSA) = b1 + b2M + b3M^2 + (b4 + b5M)\log\sqrt{Rjb^2 + b6^2} + b7S_s + b8S_A + b9F_N + b10F_R + \varepsilon\sigma \quad (3)$$

In Equation 3, S_S and S_A take 1 for soft (Vs_{30} < 360 m/s) and stiff soil sites, otherwise zero, rock sites being defined as having Vs_{30} > 750 m/s. F_N and F_R take the value of unity for normal and reverse faulting earthquakes respectively, otherwise zero; ε is the number of standard deviations above or below the mean value of log(PSA) and σ is the value of variability of inter-event ($\sigma_{\square}$) and an intra-event ($\sigma_{\square\square}$. The total standard deviation σ is calculated by the square root of the sum of their squares in Equation 4 (Akkar and Bommer, 2010).

$$\sigma = \sqrt{\sigma 1^2 + \sigma 2^2} \quad (4)$$

Since we are interested in calculating the PGA from the equation of pseudo spectral acceleration, the values of b coefficients are taken for the period T_i=0, as follows:

b_1=1.43525; b_2=0.74866; b_3=-0.0652; b_4=-2.7295 ; b_5=0.25139 ; b_6=7.74959;
b_7=0.0832; b_8=0.00766; b_9=-0.05823; b_{10}=0.07087; σ=0.2611 ; ε=0.1056.

Table 1 reviews the existing simplified Newmark equations and an alternative of Arias intensity to be calculated instead of PGA in the landslide displacement.

Table 1. Review of the existing simplified Newmark models and their associated parameters.

No.	Equation	Developed by:
(5)	$\text{Log DN} = 0.90 + \log[(1 - \frac{ac}{amax})^{2.53} (\frac{ac}{amax})^{-1.09}] +- 0.30$	Ambraseys et al. (1988)
(6)	$\text{Log DN}=\log[\frac{D_N g}{a_{max} N_{eq} T^2}] = 0.22 - 10.12(\frac{ac}{amax}) + 16.38(\frac{ac}{amax})^2 - 11.48(\frac{ac}{amax})^3$	Yegian et al. (1991)
(7)	(a) $\text{Log DN} = 1.521 \log Ia - 1.993 \log ac - 1.546$ (b) $\text{Log (Ia)} = M - 2\log\sqrt{R^2 + h^2} - 4.1$	Jibson (1993)
(8)	$\ln(I_a) = c1 + c2(M - 6) + C3\ln(M - 6) + c4\ln(\sqrt{R^2 + h^2}) + (s11 + s12(M - 6))S_c + (S21 + S22(M - 6))S_D + f1F_N + f2F_R$	Travasarou et al. (2003)
(9)	$-2.710 + log10[(1 - {}^{ac}/_{amax})^{2.335} * ({}^{ac}/_{amax})^{-1.478}] + 0.424 * M$	Jibson (2007)

Equation 5 suggests an approach based on the sets of regression equations of actual ground motion recorded as the function of a_{max} (peak ground acceleration) and a_c (critical acceleration) (Ambraseys et al. 1988). The second type of simplified equation was introduced by Yegian et al. (1991), suggesting that PGA cannot be a sole descriptor of the behavior of ground motion to calculate the displacement in Equation 6. They considered frequency content and duration as important parameters to calculate the median normalized Newmark displacement. In Equation 6, a_c and a_{max} account for the critical acceleration and the peak ground acceleration, N_{eq} is an equivalent number of cycles and T is the predominant period of the input motion. Recognizing that the PGA tends to correlate poorly with earthquake damage, there were some suggestions to develop an equation based on the Arias Intensity (Ia), a measure of the intensity of shaking which comes from the acceleration of transient waves. Jibson (1993) suggested Equation 7a, the regression equation by the calibration of the double-integration of 11 acceleration time histories, including 10 time histories of Californian earthquakes, with arias intensities with the value of equal or less than 10 m/s over a range of critical acceleration values (0.02-0.40g). The attenuation relationship for Arias intensity can be calculated based on Equation 7b. In this equation, R accounts for the closest distance to the rupture plane in km and h stands for fictitious hypo central depth in km. A more recent equation to calculate the arias intensity, was developed by Travasarou et al. (2003), which is an empirical equation calculated from the nonlinear regression analysis as shown in Equation 8. The coefficients of the empirical equation for Arias intensity have the following values: c_1=2.800, c_2=-1.981, c_3=20.72, c_4=-1.703, h=8.78, s11=0.454, s_{12}=0.101, s_{21}=0.479, s_{22}=0.334, f_1=-0.166, f_2=0.512. F_N, F_R, S_C, and S_D take the value of unity for normal and reverse faulting earthquakes respectively, otherwise zero. The last equation has been suggested again by Jibson (2007), which balances between critical and maximum acceleration and earthquake intensity measure to calculate the displacement, as shown in Equation 9. Among all the equations that are already explained, for the illustration purposes, we chose the Equation 9 to calculate the maximum displacement of each cell of the slope for the given mechanical parameters, PGA, and, earthquake magnitude. Although, it is relatively straightforward to apply any of the equations that follow this type of slope-performance zonation, we believe that Equation 9 takes into account the mechanical parameters of the slope as an indicator of physical characteristic of the slope failure, and the ground shaking parameters as an intensity measure of the earthquake and thus a good indicator of the slope failure mechanism.

2.3 Procedure to develop the landslide footprint model within CA modeling

The CA is initiated by evaluating the susceptibility of cells to fails during earthquake shaking from the simplified Newmark method. The landslide then propagates by iterations depending, for each cell, on the state of its neighbor cells, the outflow computation from the cells giving the evolution of the landslide. The CA stops when the slope gradient in each cell becomes less or equal to the stable slope or when all the materials in the cells are eroded away. Each Sandpile avalanche is equivalent to one landslide. The landslide footprint model is developed based on the following procedure:

i. An idealized topography (XYZ data or raster) is defined as a square grid to calculate the maximum slope angle using tangent inverse equation in the binned cells. The topographic data for the model implementation in a real-site condition is acquired from the geodetic portal of ETH Zurich (https://geodata.ethz.ch).
ii. Fault segments are added to the system characterized by the fault's length, dipping, and depth. Earthquakes footprints are then produced in the same grid system in terms of PGA as a function of the earthquake magnitude (Mw), Rjb (distance from the surface projection of the rupture to the site) and Ti = 0 sec following the Ground Motion Prediction Equation (GMPE) of Akkar et al. (2014).
iii. The effect of the rainfall intensity is added to the system with the saturated thickness of the slab (hw). The static factor of safety is calculated for the terrain, using the slope characteristics (i.e., soil unit weight, effective cohesion, effective friction angel, etc.). Note that the terrain with factor of safety (F_s) larger than 1.5 is considered to be unconditionally stable; with $1<F_s<1.5$, the terrain is conditionally stable, and with $F_s<1$, the terrain is unconditionally unstable.
iv. The simplified Newmark model is applied to the system to calculate the displacement of each cell. We use Equation 9, which balances PGA, critical acceleration shown in Equation 1, and the earthquake intensity measure.
v. The landslide flow starts in those cells whose initial displacement due to the combined effect of rain and earthquake are higher than the boundary limit displacement. Landslides are generated by first identifying target grid cells that exceed a boundary limit displacement (Newmark displacement ≥ 5cm)- based on the

critical acceleration (a_c) necessary to initiate slope failure (Wieczorek et al. 1985; Jibson et al. 2000; Godt et al. 2008).

vi. In this step the maximum stable slope gradient with the current geo-mechanical properties (step iii) under the specified earthquake loading is calculated. Then the difference between the values of landslide angle and the maximum stable angle, distinguishes the amount of the "gradient change". We relate the amount of displacement in cells to this value of the gradient change, considering the fact that the values of slope gradients, which are higher than the " maximum stable slope", produce displacements more than the critical displacement (5 cm). At each iteration, this procedure shapes a new topography and stores a new landslide footprint. The loop ends, either when the slope gradient tends to the stable topography, or when there is no more material to be moved away.

So far, the landslide is assumed to be composed of material from the above the height of the soil (h). Different approaches will be tested in the future to define different types of landslides, for example considering the case where only the soil from the original unstable area can flow, or the case where the thickness or strength of the shallow soil varies for different slopes.

3. PRELIMINARY RESULTS AND INTERPRETATION

We modeled the landslides triggered by an earthquake and heavy rain based on the concept of Newmark displacement for the case of a large earthquake (Mw=6.5) and for different saturation conditions including dry, half saturated, and saturated condition. This analysis has been performed for the topography defined for the virtual area concept (Fig. 2a). Fig. 3a shows that for the values of higher slope gradient, the factor of safety passes from stable to critical and finally unstable condition. It also compares the amount of stable slope for different saturation conditions. Fig. 3b shows the amount of critical displacement through different stability conditions based on the combined effects of geotechnical properties of the slope and the earthquake triggering.

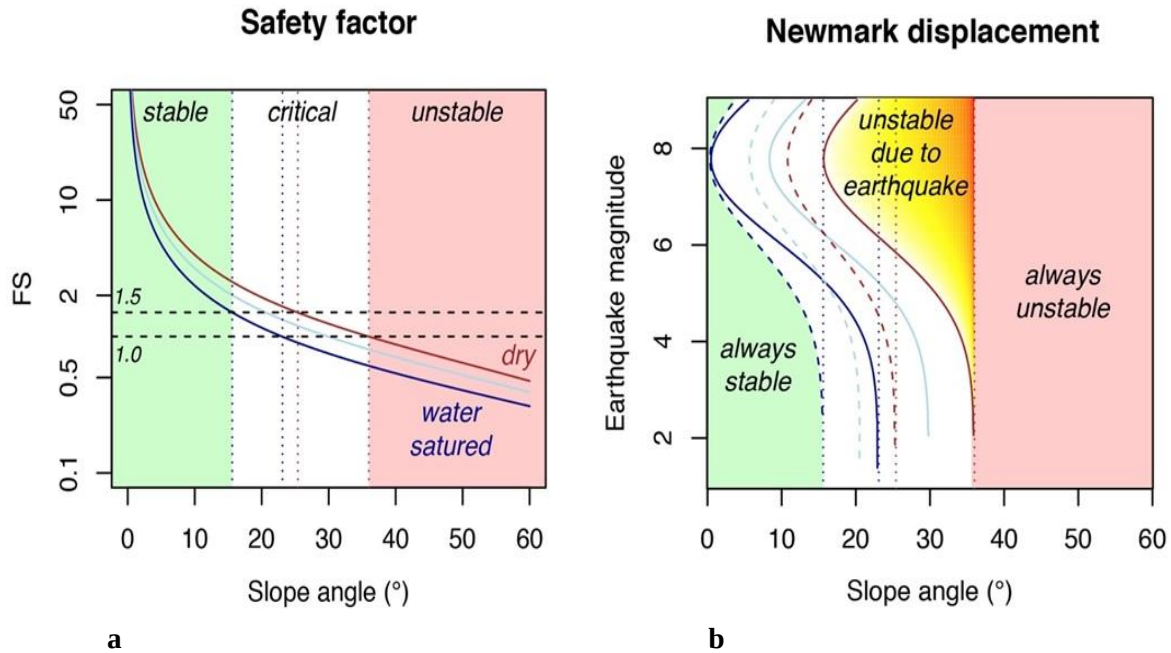

Figure 3. a: Safety factor versus slope gradient for different saturation conditions; b: Newmark displacement as a combined effect of earthquake magnitude and slope angle.

We applied the CA model over the topography defined in the virtual area, with the same assumption of the earthquake magnitude in the half saturated condition with the 10 meters thickness of slab, and estimated the landslide footprint with the varying depth. The animation created for this model showed an expected flow from plateau to the river basin. The footprint at a given iteration is shown in Fig. 4.

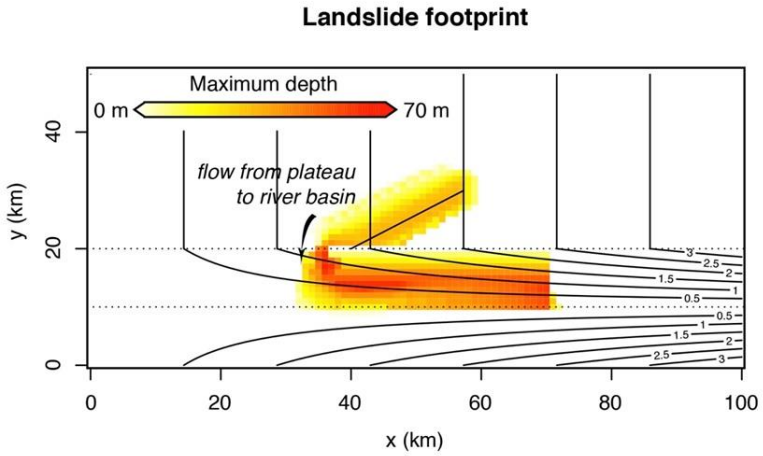

Figure 4. Landslide footprint and flow from plateau to the river basin for the earthquake of magnitude 6.5, in a half water saturated soil tested in the virtual area.

The CA model described above is applied again over the regions with the higher risks of landslide in Switzerland including areas, which previously have been affected through history by the combined impacts of earthquake and water saturation due to heavy rainfalls. For illustration, we picked here an area in the Mattertal valley (St. Niklaus) in the canton of Valais, Switzerland (the steep valley that runs from Stalden to Zermatt and is surrounded by some of the highest summits in the Alps, such as Dom and Weisshorn). The city of St. Niklaus sits inside this valley and has an elevation of 1,120 meters A.S.L and a population of 2,291 (STAT-TAB 2015). The topography data has been extracted from GeoVITe project, "Geodata Visualization and Interactive Training Environment", which offers an easy-to-use online access to the most important Swisstopo geo datasets for research and educational purposes at ETH Zurich. We obtained the data from the DHM 25-Matrix model which is essentially based on the Swiss National Map 1:25 000 and the height matrix with 25 m grid is interpolated from the basis model (Swisstopo 2005). Fig. 5 shows the digital elevation model of the DHM 25 matrix model type of the Mattertal valley in Swiss X and Y coordinates.

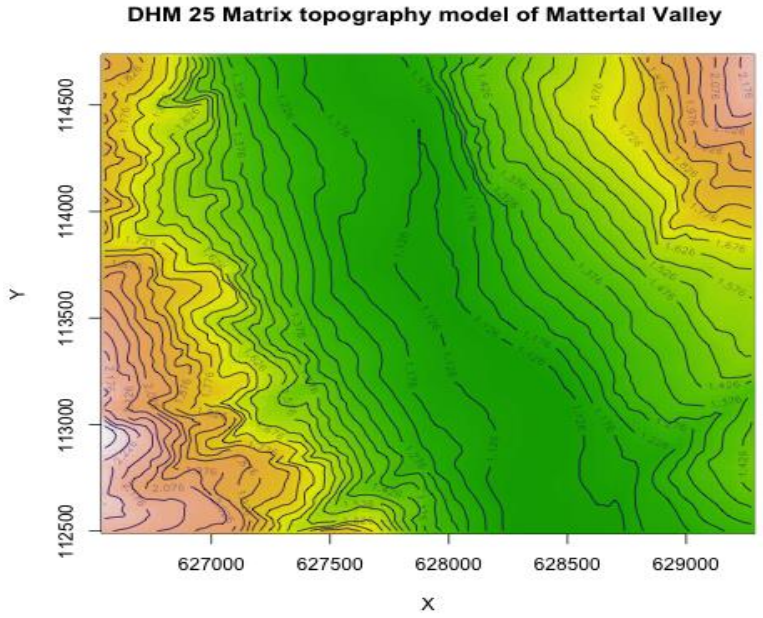

Figure 5. DHM 25 matrix topography model of the tested real-site conditions, Mattertal valley, Switzerland.

As a follow-up to the analysis on the virtual area topography, a Newmark displacement threshold is set for the initiation of the landslide to calculate the matrix of the most stable slope gradient (Wieczorek et al. 1985; Jibson et al. 2000; Godt et al. 2008). The boundary condition is set on the soil parameters and the fault activity due to the imposed earthquake of magnitude 6.5 on the hypothetic fault segment, in a half saturated condition

with 10 meters of the thickness that can be moved away. The cellular automaton is applied in a real test condition. The amount of maximum acceleration due to earthquake on projected fault segment is shown in Fig. 6a. The landslide footprint and the accumulation pattern of the debris in the downslope fan through different ravines are shown in Fig. 6b. Scale bar shows the depth of the accumulation of the debris in the fan.

Compared to aerial images, this pattern shows that such a landslide would directly threaten some villages. However, the Newmark method is subject to high uncertainties (e.g., Table 1) and different landslide footprints can be obtained depending on the selected equation. Moreover, comparison with historical footprints, results from past-published simulations and expected footprint size distributions has yet to be made to validate the proposed CA model. At this stage, ongoing simulations (e.g., Fig. 6b) appear "visually reasonable" but this needs to be confirmed by some statistical tests.

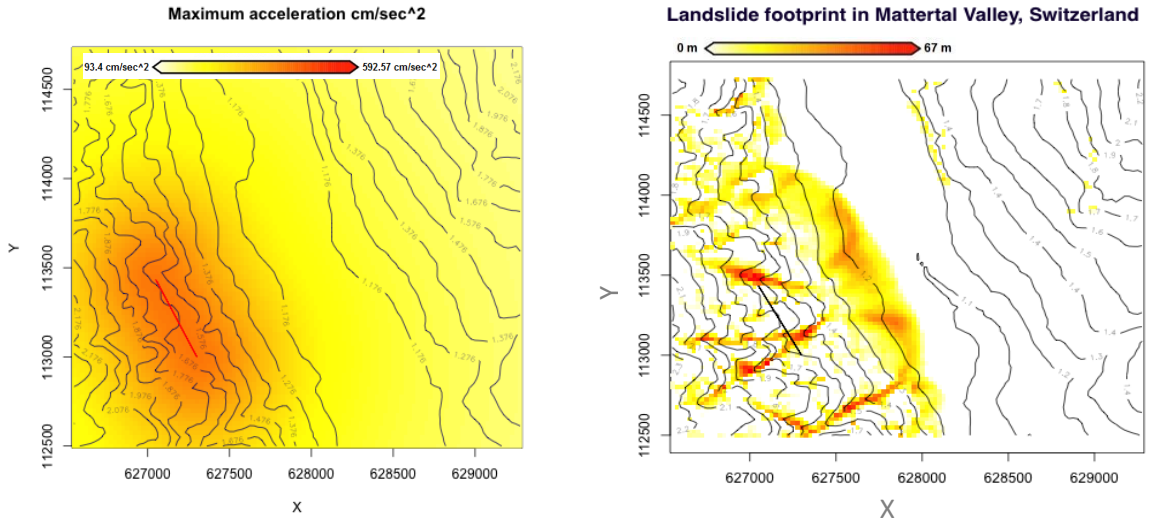

Figure 6. Hypothetical scenario of landslide triggered by an earthquake a: Values of maximum acceleration (PGA) for an earthquake (Mw=6.5) occurred on a segment of the thrust fault in Mattertal valley, Switzerland; b: Landslide footprint tested in the real-site condition in - Mattertal Valley, Switzerland.

4. CONCLUSION

An innovative cellular automaton has been developed to estimate the landslide footprint based on the Newmark slope stability analysis considering earthquake shaking and different saturation conditions as an indicator of the rainfall level. The model has been tested in a virtual area and an area in Switzerland prone to landslides, in Mattertal valley, Valais canton. We described the steps of the CA model and showed that preliminary results are encouraging but have yet to be validated. In the next phase, we will investigate the validity of the model by testing different metrics, such as the slope of the landslide frequency-size distribution and the maximum spatial extent of landslides as a function of earthquake magnitude. We plan to run our model coupled with various geologic maps and generate modeled landslides inventories for landslide risk analysis in the GenMR framework. The final goal of this study is to go towards a unified multi-risk picture of Switzerland by combining this work with other ongoing efforts in the modeling or risk at dams and geo-energy sites in the country.

5. ACKNOWLEDGMENT

This paper describes a current research plan of the NRP70 WP5 PhD project on "multi-risks and interdependencies" in ETH Zurich, started in January 2015 and related to the Swiss Competence Center for Supply of Electricity (SCCER SoE) T4.1 "Risk, safety and societal acceptance". The PhD is planned to be continued until January 2018, and complementary results will be added to the current state of the research.

6. REFERENCES

Akkar S, Bommer JJ. Empirical equations for the prediction of PGA, PGV, and spectral accelerations in Europe, the Mediterranean region, and the Middle East. Seismological Research Letters. 2010 Mar 1;81(2):195-206.

Akkar S, Sandıkkaya MA, Bommer JJ. "Empirical ground-motion models for point-and extended-source crustal earthquake scenarios in Europe and the Middle East". Bulletin of earthquake engineering. 2014 Feb 1;12(1):359-87.

Ambraseys NN, Menu JM. Earthquake- induced ground displacements. Earthquake engineering & structural dynamics. 1988 Oct 1;16(7):985-1006.

Bak P, Tang C, and Wiesenfeld K, "Self-Organized Criticality," Physical Rev. A, Vol. 38, No. 1, 1 July 1988, pp. 364–374.

Fritsche S, Fäh D, Schwarz-Zanetti G,"Historical intensity VIII earthquakes along the Rhone valley (Valais, Switzerland): primary and secondary effects". Swiss Journal of Geosciences. 2012 Jun 1;105(1):1-8.

Godt J, Şener-Kaya W, Lu N, Baum RL. "Stability of infinite slopes under transient partially saturated seepage conditions". Water Resources Research, 2012, v. 48, no. 5,p. W05505. doi: 10.1029/2011WR011408.

Harp, Edwin L., and Jibson, Randall W., 1995, Inventory of landslides triggered by the 1994 Northridge, California earthquake: U.S. Geological Survey Open-File Report 95-213.

Jibson RW. "Regression models for estimating coseismic landslide displacement." Engineering Geology. 2007 May 22;91(2):209-18.

Jibson RW, Harp EL, Michael JA. "A method for producing digital probabilistic seismic landslide hazard maps": Engineering Geology, 2000, v. 58, no. 3–4, p. 271-289. doi:10.1016/S0013-7952(00)00039-9.

Jibson RW. "Predicting earthquake-induced landslide displacements using Newmark's sliding block analysis." Transportation Research Record (Transportation Research Board), 1993: 9-17.

Komendantova N, Mrzyglocki R, Mignan A, Khazai B, Wenzel F, Patt A, Fleming K. "Multi-hazard and multi-risk decision-support tools as a part of participatory risk governance: Feedback from civil protection stakeholders." International Journal of Disaster Risk Reduction (Elsevier Ltd.) 8 (2014): 50-67.

Malamud BD, Turcotte DL. "Cellular Automata Models Applied to Natural Hazards". Computing in Science & Engineering. 2000 May 1; 2(3):42-51.

Matos J, Mignan A, Schleiss, A J. "Vulnerability of large dams considering hazard interactions. Conceptual application of the Generic Multi-Risk framework", Proceedings of the 13th ICOLD Benchmark Workshop on the Numerical Analysis of Dams, Lausanne, Switzerland, 9-11 September 2015. 2016, pp. 285-292

Mignan .A, Komendantova N, Scolobig .A, Fleming K. "Multi-Risk Assessment and Governance", Handbook of Disaster Risk Reduction and Management, World Sci. Press & Imperial College Press, London (2016).

Mignan A, Wiemer S, Giardini D. "The quantification of low-probability–high-consequences events: part I. A generic multi-risk approach." Nat Hazards (Springer), April 2014: 1999

Mignan, A., Scolobig, A., Sauron, A. "Using reasoned imagination to learn about cascading hazards: a pilot study", Disaster Prevention and Management, 25(3), 2016 b, doi: 10.1108/DPM-06-2015-0137, in press

Newmark NM. "Effects of earthquakes on dams and embankments." Fifth Ranking Lecture, University of Illinois, Urbana, Illinois., 1965, 139-160.

Pickover CA. "The math book: from Pythagoras to the 57th dimension, 250 milestones in the history of mathematics". Sterling Publishing Company, Inc.; 2009.

STAT-TAB, Swiss Federal Statistic Office. "Ständige und Nichtständige Wohnbevölkerung nach Region, Geschlecht, Nationalität und Alter (German) accessed 31 August 2015." Statistik Schweiz. http://www.bfs.admin.ch/bfs/portal/de/index/themen/02/03/blank/data/gemeindedaten.html

Swisstopo. Federal office of topography (Swisstopo). June 2005. http://www.swisstopo.admin.ch/internet/swisstopo/en/home/products/height/dhm25.html.

Travasarou T, Bray JD, and Abrahamson NA. "Empirical attenuation relationship for Arias Intensity." Earthquake engineering and structural dynamics (Earthquake Engng Struct. Dyn) 32 (2003): 1133–1155.

Wieczorek GF, Wilson RC, Harp EL. "Map showing slope stability during earthquakes in San Mateo County, California": U.S.Geological Survey Miscellaneous Investigations Map, 1985 ,I-1257-E, scale 1:62,500.

Yegian MK, Marciano EA, Ghahraman VG,. "Earthquake-induced permanent deformations: probabilistic approach." (Journal of Geotechnical Engineering,ASCE) 117, no. 1 (January 1991): 35-50.